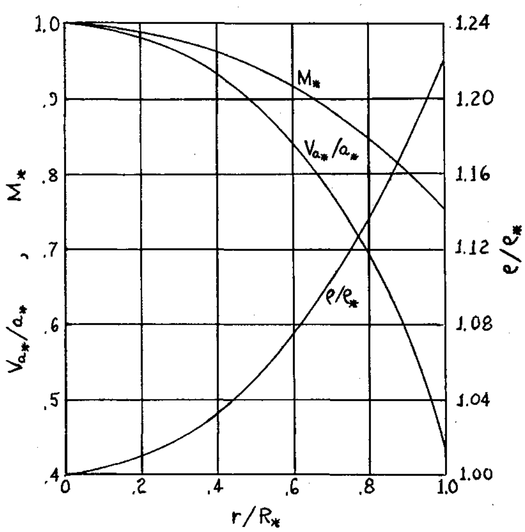

Fig. 2 Property distributions at nozzle throat.

which reduce to the usual one-dimensional results for no spin

Therefore, substituting (10) into (6) yields the complete expression for the axial velocity distribution at the nozzle throat:

$$V_{a*}{}^2 = a^{*2} - \omega_0{}^2 \left(\frac{R_0}{R_*}\right)^2 \left[2\left(\frac{R_0}{R_*}\right)^2 - 1\right] r^2 \qquad (11)$$

Setting $V_a{}^{*2} = 0$ in Eq. (11) yields

$$V_{t_0}{}^2 = 2g\gamma RT_0/(\gamma + 1)[2(R_0/R^*)^2 - 1] \qquad (12)$$

which defines the limiting tangential velocity at the grain surface for which this method of analysis is applicable. For values of V_{t_0} greater than those defined by Eq. (12), the possibility of reverse (upstream) flow toward the wall of the nozzle throat is indicated. Such a phenomenon was observed in a number of swirling flow experiments described in Ref. 3.

Sample Results

Assuming $T_0 = 4500°\text{R}$, $\gamma = 1.25$, $\omega = 300$ rps, $R_0/R^* = 17.32$, and $R^* = 0.0035$ ft, Fig. 2 gives the normalized velocity, density, and Mach number distributions at the nozzle throat. From these, the (numerically) integrated average velocity is found to be only 74.6% of the (sonic) velocity at the centerline, the average density 10.9% higher than at the centerline, and the average Mach number 0.877.

The normalized mass flow rate is calculated from

$$\dot{m}_\omega/\dot{m} = (\textstyle\int \rho V dA_*)/\rho_* V_* A_* \qquad (13)$$

and since the critical parameters are defined, may be rewritten as

$$\frac{\dot{m}_\omega}{\dot{m}} = \frac{2}{R_*}\int_0^{R_*}\left(\frac{\rho}{\rho_*}\right)\left(\frac{V_{a*}}{a_*}\right)\left(\frac{r}{R_*}\right) dr \qquad (14)$$

and numerically integrated to yield (for this example) a mass flow only 83.9% of that which would be experienced without spin.

The change in motor operating pressure for a change in nozzle throat area is calculated from

$$P_\omega/P = (A_*/A_{*\omega})^{1/(1-n)} \qquad (15)$$

If it is assumed that the reduction in efflux obtained from Eq. (14) is equivalent to a corresponding reduction in (effective) nozzle throat area, (15) may be rewritten as

$$P_\omega/P = (\dot{m}/\dot{m}_\omega)^{1/(1-n)} \qquad (16)$$

Figure 3 gives P_ω/P as a function of n for the example cited.

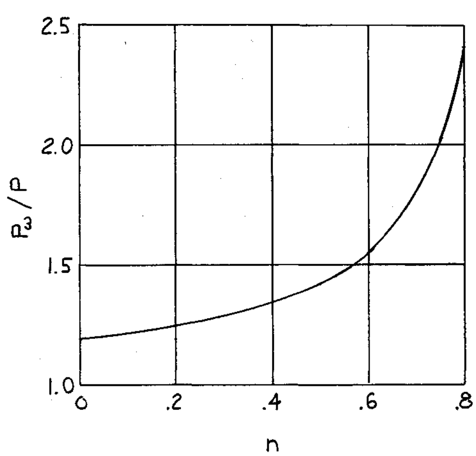

Fig. 3 Pressure exponent influence on combustion pressure.

Conclusions

By assuming that the energy and angular momentum of a differential ring of propellant gasses are conserved as this body of gas proceeds isentropically through a nozzle, it is shown that, as a function of roll rate, there can be a considerable reduction in nozzle efflux, with a corresponding increase in motor operating pressure.

For end-burning grains, Eq. (11) indicates that spin effects on nozzle performance should be less pronounced with higher-energy propellants (larger a^*) and lower design combustion pressures (R_0/R_*).

References

[1] Bastress, E. K., "Interior ballistics of spinning solid-propellant rockets," J. Spacecraft Rockets **2**, 455–457 (1956).

[2] Binder, R. C., *Fluid Mechanics* (Prentice-Hall Inc., Englewood Cliffs, N. J. 1955), Chap. X, p. 167.

[3] Binnie, A. M., Hookings, G. A., and Kamel, M. Y. M., "The flow of swirling water through a convergent divergent nozzle," J. Fluid Mech. **3**, 261–274 (1957).

Erratum: Minimum Energy Deorbit

Barry A. Galman*
General Electric Company, Philadelphia, Pa.

[J. Spacecraft Rockets **3**, 1030–1033 (1966)]

THE last term of Eq. (13) should be

$$-4K/V_0{}^2\}^{1/2})$$

Received August 15, 1966.

* Manager, Dynamic Analysis, Manned Orbiting Laboratory Department. Member AIAA.